JOURNAL OF SYNCHROTRON RADIATION

ISSN 1600-5775

On the advantages of operation in second-order diffraction of blazed gratings in soft X-ray monochromators

Werner Jark*

Elettra – Sincrotrone Trieste SCpA, SS 14 km 163.5 in AREA Science Park, Basovizza, 34149 Trieste, Italy. *Correspondence e-mail: jark@elettra.eu

Received 12 June 2019
Accepted 1 July 2019

Edited by S. Svensson, Uppsala University, Sweden

Keywords: diffraction grating; soft X-rays; diffraction efficiency; second-order diffraction; soft X-ray monochromator.

The fact that a diffraction grating can provide twofold-smaller bandwidth when operated in second-order diffraction is long known and applied routinely in the laboratory for spectroscopy in the visible and ultraviolet spectral range. A similar routine operation in monochromators for the soft X-ray range is not reported yet. This study will thus address the feasibility of efficient diffraction of soft X-rays in the second order at reflection gratings when operated at grazing angles of incidence. The related systematic study could make profitable use of a recently introduced simple analytical equation for the prediction of the diffraction efficiency of blazed gratings with an ideal sawtooth profile. The predictions are then verified by use of rigorous calculations. The principle finding is that, by operation of gratings with lower groove densities, and thus with higher efficiencies, in higher order diffraction, one can extend the tuning in existing instruments with mechanical/optical limitations to larger photon energies. The performance in terms of transmission and spectral resolving power can be very similar to the performance of a grating with a larger groove density, which would otherwise have to be used for accessing the same energy range. This would allow operation of a single highly efficient grating over a larger photon energy interval at a modern synchrotron radiation source, *e.g.* from 0.3 to 2.2 keV. Without any requirement for a sophisticated grating exchange scheme, a related instrument promises to be sufficiently stable for the needs imposed by the improvements in source point stability at diffraction-limited storage rings.

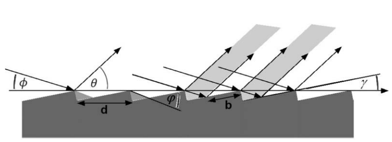

1. Introduction

As long as the operation of monochromators for the soft X-ray range (0.3–8 keV) is projected only up to the limit in photon energy of about 2–2.5 keV, reflection gratings are almost exclusively employed for the dispersion of the incident radiation at shallow angles of deflection. The selection of the wavelength λ by use of these devices, as presented in Fig. 1, is then based on the grating equation (see *e.g.* Hutley, 1982)

$$n\lambda = d(\cos\phi - \cos\theta), \qquad (1)$$

where n (an integer) is the order of diffraction, d is the grating periodicity and ϕ and θ, with $\theta \neq \phi$, are the angles of grazing incidence and of grazing diffraction, respectively. The wavelength (λ) and photon energy (E) are related via λE = 1.23985 nm keV. Here the sign convention is $n > 0$ when $\theta > \phi$, *i.e.* when the respective diffraction order is observed between the incident and the specularly reflected beam. The minimum achievable source-size-limited spectral bandwidth is obtainable from the derivative of equation (1),

$$\frac{\partial}{\partial\phi}\lambda\Delta\phi = \frac{\partial}{\partial\phi}\frac{d}{n}(\cos\phi - \cos\theta)\Delta\phi = \frac{d}{n}\sin\phi\Delta\phi, \qquad (2)$$

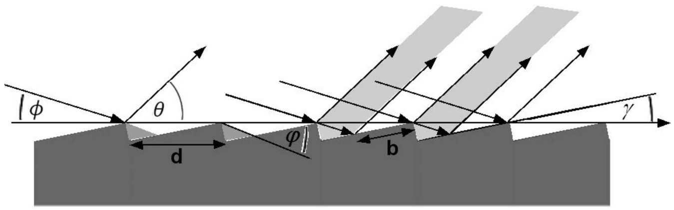

Figure 1
Diffraction of a radiation beam striking a diffraction grating with periodicity d and an angle of grazing incidence of ϕ, and which is diffracted by an angle of θ away from the surface. The situation is presented for a blazed grating with blaze angle γ. In the first two grooves on the left, grey triangles indicate up to which inclination the sawtooth angle can deviate from a right angle without affecting the diffraction process. Here the angle φ is referred to as the anti-blaze angle.

where $\Delta\phi$ is the intrinsic beam angular divergence limited by the finite source size s and given by the ratio of this size s and the source distance L. According to equation (2) the use of the second ($n = 2$) or even higher orders can then help to reduce the achievable spectral resolution at least twofold (see, for example, Born & Wolf, 1980). This strategy is regularly applied when the incident light from laboratory line sources, emitting smaller photon energies from the visible spectral range up to the vacuum ultraviolet (VUV), is dispersed at close to normal incidence. In this case, interferences by integer multiples of the respective wavelength need to be absent or need to be eliminated by appropriate means such as filters. As far as synchrotron radiation at larger photon energies in the soft X-ray range is concerned, the latter suppression strategy for the principle diffraction order with filters could be used as well at bending-magnet sources, which emit a continuous spectrum. Instead, the use of undulators would be more favourable as they emit a line spectrum which is even tunable. Nevertheless, for routinely operated monochromators for the soft X-ray range the use of the first order ($n = 1$) is reported almost exclusively for the monochromatization. The reason for this lies in the flexibility, which is provided in monochromators for the soft X-ray range in comparison with solutions for normal incidence. The optics in soft X-ray monochromators needs to be operated at grazing angles of incidence, and the most flexible configuration for the monochromatization is achieved when a double bounce is realized in a plane-mirror plane-grating pair, in such a way that the deflection angle in the dispersion process can be varied while the exiting monochromatic beam remains stationary in position and angle. This concept was introduced by Kunz *et al.* (1968) for use in combination with plane optics and gratings with constant periodicity and is discussed in detail by Petersen *et al.* (1995). When such a pair is operated in a divergent incident beam, the deflection angle variation needs to be restricted almost always to a single operation curve on which the related aberrations can be kept constant. Petersen *et al.* (1995) reported on the monochromator operation with $n = 2$ under such conditions and found an improvement in the spectral resolution which, however, remained far from a factor of two. Later, Follath & Senf (1997) introduced a collimation mirror in front of the mirror/grating pair, which eliminated most of the aberrations originating in the grating with constant groove density. Then, in a collimated beam, the deflection angle at a plane grating with constant periodicity can be chosen freely. Consequently, this can be used in order to vary the spectral resolution, as shown by Follath & Senf (1997) and by Follath (2001). Such a variation can be by more than a factor of two, and then use of the second order ($n = 2$) does not provide any advantage in this respect; hence, this type of operation in the second order will not be discussed here.

The second-order diffraction is always discussed in soft X-ray monochromators, when the higher order suppression capability is the important parameter. In this case, equation (1) indicates that all integer fractions of the principle wavelength can be diffracted into the same direction. Such photons can thus be transmitted through a monochromator as an undesired impurity or contamination when a source is emitting photons also at the respective wavelengths (*e.g.* a bending magnet at synchrotron radiation sources). This study will then address the question of whether the higher-order contamination in conditions of poor higher-order suppression can eventually offer advantages over the normal first-order operation of the monochromator.

2. Conditions for 'higher-order operation' of soft X-ray gratings

As laminar grating profiles have intrinsic higher-order suppression capabilities (see, for example, Follath & Senf, 1997), only gratings with a sawtooth or blazed profile will be considered in this discussion. The findings from a recent study by Jark (2019) can then be used for the present discussion. In the latter study, and whenever possible here, the small-angle approximations for the sine and cosine functions are used. It was shown by Jark (2019) that the diffraction efficiency of a blazed grating with a perfect rectangular sawtooth profile in bulk material can be approximated with little error compared with more adequate rigorous calculations by use of an analytical equation. For the orders $n = 1$ and $n = 2$, to which the present discussion will be limited, the efficiency can be calculated by the use of three independent multiplicative factors,

$$e_{n=1,2} = R(\lambda, \phi + \theta)\frac{\phi}{\theta}S^2_{n=1,2}(\lambda, \phi, \theta, \gamma), \qquad (3)$$

where $R(\lambda, \phi + \theta)$ refers to the reflectivity of the coating, ϕ/θ refers to the applied geometry, and only the structure factor $S^2_{n=1,2}(\lambda, \phi, \theta, \gamma)$ contains information about the grating profile. The exact form of the latter for a grating with an ideal sawtooth profile was derived by Lukirskii & Savinov (1963). An approximation for the structure factor for practical applications is discussed in Appendix *A*. It was shown by Jark (2019) that it is here more convenient to use as the variable the angle of grazing deflection $\phi + \theta$. With γ being the blaze angle of the grating, *i.e.* the shallow angle of inclination of the sawtooth profile with respect to the substrate surface, in the condition $\phi + \gamma = \theta - \gamma$ the intensity diffracted into a specific diffraction order can be considered to have been specularly reflected at the inclined grating grooves. This condition is thus called the blaze maximum condition (BM), in which case the structure factor is maximum with $S^2_{n=1,2}(\lambda, \phi, \theta, \gamma) = 1$. The latter factor is valid for both beam paths, *i.e.* when the incident radiation follows the trajectory presented in Fig. 1 and when it follows the reversed trajectory. It can be shown that the related blaze maximum wavelengths are given by

$$\lambda_{\rm BM} = \frac{d}{n}\gamma(\theta + \phi)_{n,{\rm BM}}. \qquad (4)$$

The geometrical factor $\phi/\theta = G$ is always $G < 1$, for which reason the diffraction efficiency can never equal the reflection coefficient for the inclined surface but is reduced even in blaze maximum to at best

$$e_{\rm BM} = R(\lambda, \phi + \theta)G. \qquad (5)$$

The discussion will herein be limited to gold coatings, which are favoured for reflection gratings for the soft X-ray range. Jark (2019) then showed for the photon energy range considered here (0.3–2.5 keV) that, as long as one does not consider the structure factor, each groove density $1/d$ of an Au-coated grating is associated with a specific geometrical factor G, *i.e.* a possible grating operation curve, close to which the maximum of the efficiency is observed. According to Jark (2019), such operation curves are given by

$$(\phi + \theta)_G = \left(\frac{2\lambda}{d}\right)^{1/2}\left(\frac{1+G}{1-G}\right)^{1/2}. \qquad (6)$$

This operation mode with constant G coincides with the original operation mode of the plane-grating monochromator as discussed by Petersen (1982). He introduced the fixed-focus parameter $c_{\rm ff} = 1/G$, which in an incident divergent beam needed to be kept rigorously at a value of $c_{\rm ff} = 2.25$, limiting the optimum monochromator operation to a single working curve. Even though the use of a collimated incident beam permits us to abandon this operation mode, the concept of operation with constant $c_{\rm ff}$ is still maintained; however, the fixed-focus constant $c_{\rm ff}$ is varied according to the user needs, either good higher-order suppression or high spectral resolution.

Jark (2019) found (empirically) for the best efficiency for a gold coating a linear dependence between the latter fixed-focus constant and the grating groove density ($1/d$), with the relation

$$c_{\rm ff} = \frac{1}{G} = 1.1 + \frac{913\,{\rm nm}}{d} \qquad (7)$$

for gratings with groove densities between 50 mm^{-1} and 1200 mm^{-1}, the latter being the current most favoured groove density. As a consequence, when the grating is used at undulators of length D at a diffraction-limited storage ring, the spectral resolving power RP is constant for any $c_{\rm ff}$ value and can be calculated ideally for first-order diffraction as

$$\left(\frac{\lambda}{\Delta\lambda}\right)_{n=1} = {\rm RP} = 2\left(\frac{1}{G^2} - 1\right)^{1/2}\frac{L}{(dD)^{1/2}}. \qquad (8)$$

When the $c_{\rm ff}$ value is chosen according to equation (7), RP increases approximately linearly with increasing groove density. These latter dependencies in equations (5), (7) and (8) are in line with previous experiences from monochromator optimizations and successive experimental verifications: the spectral resolving power is increasing with increasing groove density, while inconveniently the diffraction efficiency is decreasing in this case. According to equation (2), the spectral resolution depends on the source size s, which varies at an undulator at a diffraction-limited storage ring proportionally to $\sqrt{\lambda}$. This was considered for the derivation of equation (8); however, when it comes to second-order wavelengths in the incident beam, one needs to consider that the related source size is smaller by a factor of $\sqrt{2}$. Thus when the exit slit is properly matched to the reduced image sizes of higher-order radiation, the related spectral resolving power in such a higher-order operation scheme improves compared with operation in the first order to

$$\left(\frac{\lambda}{\Delta\lambda}\right)_n = {\rm RP} = 2\left(\frac{1}{G^2} - 1\right)^{1/2}\frac{\sqrt{n}L}{(dD)^{1/2}}. \qquad (9)$$

Instead, when the exit slit setting remains matched to the first-order source size, the spectral resolving power is given by equation (8) as well for all higher-order radiation.

The gold coating can be used efficiently and free of absorption lines up to photon energies of E = 2.2 keV (λ = 0.56 nm), where the Au M absorption edges will start to reduce severely the instrument transmission. This photon energy is still reflected with good efficiency with a beam deflection angle of 3°. Petersen (1982) thus projected the plane-grating monochromator for this minimum deflection angle, and in subsequent work this lower limit has been kept in the mechanical design of similar soft X-ray monochromators. It is now assumed to be desirable to operate the grating at the indicated limit (E = 2.2 keV, $\phi + \theta = 3°$) with the maximum of the diffraction efficiency according to equation (5). From equation (6), one obtains the wavelength down to which the deflection angle remains larger than $\phi + \theta = 3°$,

$$\lambda_{\rm min} = \frac{d}{2}(\phi + \theta)^2\frac{1-G}{1+G}. \qquad (10)$$

The result for the maximum efficiency curve according to equation (7) is plotted in Fig. 2 as the corresponding maximum photon energy $E_{\rm max}$ depending on groove density. One finds that only gratings with groove densities larger than about 600 mm^{-1} can provide their specific maximum diffraction efficiency at a photon energy of 2.2 keV or larger. The maximum diffraction efficiency is always found close to the blaze maximum for the principle order n = 1, in which case also the second order n = 2 is diffracted in blaze maximum. In this condition $S^2_{n=1}(\lambda, \theta, \phi, \gamma) = S^2_{n=2}(\lambda/2, \theta, \phi, \gamma) = 1$ and $G_{n=1} = G_{n=2}$. Then according to equation (3) the diffraction efficiencies for both order should be similarly high, when both reflection coefficients $R(\lambda, \phi + \theta)$ and $R(\lambda/2, \phi + \theta)$ are large. Fig. 2. invites us to consider a very particular operation mode. When the second-order diffraction occurs in blaze maximum at the minimum possible deflection angle at a photon energy

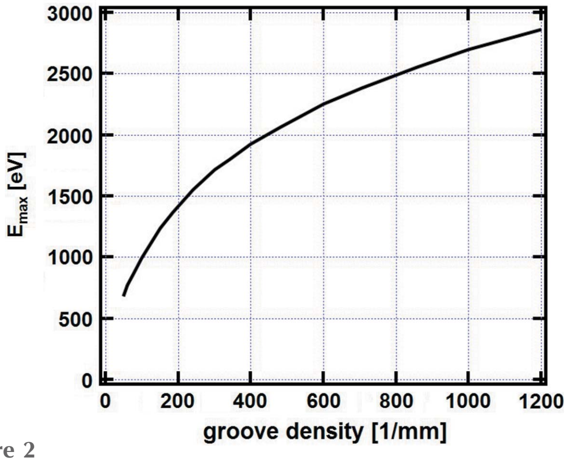

Figure 2
Dependence of the photon energy $E_{\max}$ on the grating groove density at which, according to equation (10), the maximum diffraction efficiency according to equation (7) is achieved at a deflection angle of $\phi + \theta = 3°$.

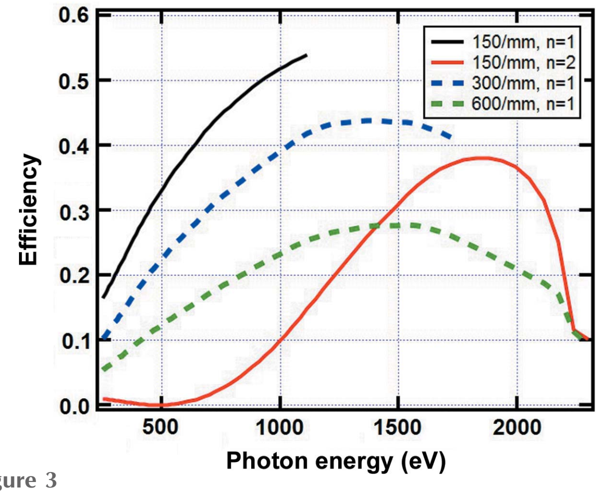

Figure 3
Rigorously calculated dependence of diffraction efficiency e (Nevière *et al.*, 1974; Schäfers, 2008) on photon energy E for the three different groove densities 150 mm^{-1}, 300 mm^{-1} and 600 mm^{-1} when operated with the constant geometrical factor G for which they provide maximum diffraction efficiency according to equation (7). The blaze angle was matched according to equation (4) to the latter condition to take place at a deflection angle of $\phi + \theta = 3°$. A perfect sawtooth profile with rectangular tip is assumed. The first-order diffraction efficiency is presented for all discussed groove densities (black line, and blue and green dashed lines), whereas the second-order diffraction efficiency is presented only for the groove density of 150 mm^{-1} (red line).

of 2.2 keV, then the blaze maximum for the first order under the same conditions is 1.1 keV. According to Fig. 2 this is the case for a groove density of around 120 mm^{-1}. We then expect that a grating with a groove density of 150 mm^{-1}, for example, as was discussed in more detail by Jark (2019), can provide highly efficient tuning up to photon energies of 2.2 keV by use of first- and second-order diffraction.

3. Discussion of the expected performance data for 'higher-order operation' of soft X-ray gratings

Without any further optimization, a comparison of the ideally achievable efficiencies has now been made, depending on the groove density and on the diffraction order. The chosen groove densities of 150 mm^{-1}, 300 mm^{-1} and 600 mm^{-1} correspond to frequently utilized fractions of the principally used groove density of 1200 mm^{-1}. The blaze angle and the geometrical factor G were chosen by use of equations (4) and (10) such that maximum efficiency was provided at or close to the photon energies according to Fig. 2. In detail, a grating with density $(1/d)$ = 600 mm^{-1} can be tuned with high efficiency to a photon energy of 2.2 keV (λ = 0.56 nm), with γ = 0.368° and G = 0.606, whereas a grating with 300 mm^{-1} can be tuned in this way only to 1.72 keV (λ = 0.72 nm), with γ = 0.24° and G = 0.782. The second order n = 2 for a density of 150 mm^{-1} can be tuned to 2.2 keV with γ = 0.184° and G = 0.785. With the same values the tuning in first order is limited to an energy of 1.1 keV (λ = 1.12 nm). A comparison of the diffraction efficiencies is presented in Fig. 3. These efficiencies are calculated rigorously by use of the differential method as presented by Nevière *et al.* (1974). The combined use of the first and the second order in combination with 150 mm^{-1} then provides the best diffraction efficiency at photon energies below 1.1 keV and between about 1.7 keV and 2.2 keV. According to equation (9), the spectral resolving power by use of this grating at higher photon energies is almost identical to the spectral resolving power of the grating with 300 mm^{-1}. The improvement compared with the operation at lower energies in first order is then 1.4-fold. The grating with 600 mm^{-1} will then provide 2-fold improvement in the spectral resolving power in the photon energy range 0.3–2.2 keV in comparison with the combinations n = 1 and 300 mm^{-1} and n = 2 and 150 mm^{-1}. This grating with 600 mm^{-1} can scan the entire indicated energy range with best performance, although only with significantly smaller efficiency compared with the lower-density gratings. As far as the gap of efficient tuning from about 1.2 keV to 1.7 keV with 150 mm^{-1} is concerned, the performance can be improved in this range in terms of efficiency by use of more adapted G factors, but at the expense of reduced resolving powers. When the same gratings are operated at a fixed deflection angle of $\phi + \theta = 3°$, the diffraction efficiencies vary as presented in Fig. 4. The previous comments on the comparison between the efficiencies in relative terms can also be applied here. From the last two figures one can then observe the following advantage for diffraction in the second order: it is a simple means of extending the tuning range of gratings with high diffraction efficiencies to larger photon energies, which might otherwise require the use of an additional grating with a different groove density.

It should also be noted that equation (4) permits the use of gratings with blaze angles twice as large for the operation at larger photon energies in the second order than in the operation in the first order in this range. This could be an advantage as the production of very shallow angles of the order of fractions of a degree is technologically challenging as discussed by Voronov *et al.* (2018).

As far as the effect of production errors in the grating profile is concerned, it is assumed that it is now possible to

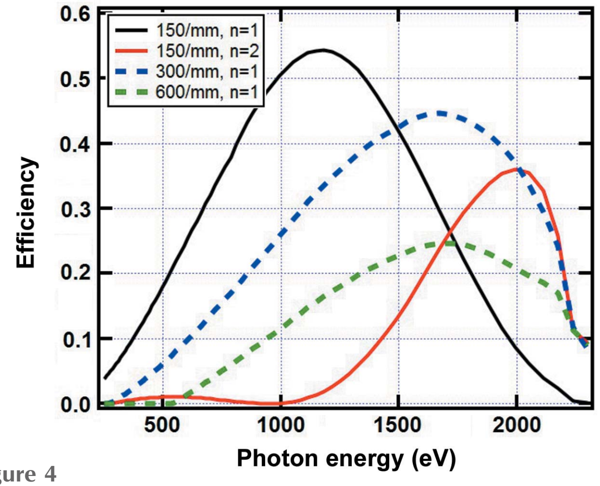

Figure 4
Rigorously calculated dependence of diffraction efficiency e (Nevière *et al.*, 1974; Schäfers, 2008) on the photon energy E for gratings with the same parameters (as indicated in Fig. 3) when operated at a constant deflection angle of $\phi + \theta = 3°$.

produce the inclined slope of the sawtooth profile to be almost perfectly flat even at very small angles, as shown by Voronov *et al.* (2018). Hence the most significant imperfection will be a not perfectly rectangular sawtooth. Ideally, the sum of the blaze angle γ and the anti-blaze angle φ, as presented in Fig. 1, should be $\gamma + \varphi = 90°$. Nevertheless, for the beam path shown in Fig. 1, the model presented by Jark (2019) is applicable for sharp sawtooth tips as long as $\varphi > \phi$, *i.e.* as long as the incident beam does not impinge onto the anti-blazed part of the profile. Sokolov *et al.* (2019) recently produced gratings with groove densities of 2400 mm^{-1} and with blaze angles $0.6° < \gamma < 1.0°$, in which the sum $\gamma + \varphi$ was as small as 1.9°. Then the sawtooth tip angle is as large as 178.1°. It is found that such a large tip angle will not alter the results of the calculations presented in Figs. 3 and 4. Then only the surface roughness will affect the diffraction efficiency. Boots *et al.* (2013) showed that the roughness will not alter the shape of the efficiency curves, but it will reduce the efficiency in second order more than first order.

4. Conclusions

In conclusion, blazed gratings with perfect profiles could be used efficiently in 'higher-order operation' in the soft X-ray range. This applies especially to gratings with lower groove densities and correspondingly larger diffraction efficiencies, for which their range of operation could then be extended to higher photon energies, which would otherwise not be possible for existing mechanical concepts with a finite minimum deflection angle.

APPENDIX *A*

In this study we intended to highlight that second-order diffraction can provide interesting performance, which is worth considering for future monochromator projects. For such purposes, the blaze maximum condition may be selected differently. One then has to recognize that the structure factor $S^2_{n=1,2}(\lambda, \phi, \theta, \gamma)$ is bell-shaped around the blaze maximum condition. A good approximation can be made with a Gaussian function as long as the deflection angle $\phi + \theta$ is significantly larger than 2γ,

$$S^2_{n=1,2}(\lambda, \theta, \phi, \gamma) = \exp\left\{-\left[\frac{n(\lambda_{\rm BM} - \lambda)}{0.54\lambda}\right]^2\right\} = \exp\left\{-\left[\frac{n(E - E_{\rm BM})}{0.54E_{\rm BM}}\right]^2\right\}. \quad (11)$$

At this point it is more convenient to discuss the properties of $S^2_{n=1,2}$ as they depend on the photon energy E. The full width at half-maximum (FWHM) of this factor for a given deflection angle is found between $E_{n,\rm FWHM,\,min} = (1 - 0.45/n)E_{n,\rm BM}$ and $E_{n,\rm FWHM,\,max} = (1 + 0.45/n)E_{n,\rm BM}$. Likewise, for a given photon energy one finds $(\theta + \phi)_{n,\rm FWHM,\,min} = (1 - 0.45/n)(\theta + \phi)_{n,\rm BM}$ and $(\theta + \phi)_{n,\rm FWHM,\,max} = (1 + 0.45/n)(\theta + \phi)_{n,\rm BM}$. So in any case the FWHM width for the normal operation with $n = 1$ is approximately twice the width of that for a 'higher-order operation' with $n = 2$.

Acknowledgements

Use of the BESSY Raytrace software package *RAY*, described by Schäfers (2008), for the calculation of the diffraction efficiencies presented here is acknowledged.

References

Boots, M., Muir, D. & Moewes, A. (2013). *J. Synchrotron Rad.* **20**, 272–285.
Born, M. & Wolf, E. (1980). *Principles of Optics*, 6th ed. Oxford: Pergamon.
Follath, R. (2001). *Nucl. Instrum. Methods Phys. Res. A*, **467–468**, 418–425.
Follath, R. & Senf, F. (1997). *Nucl. Instrum. Methods Phys. Res. A*, **390**, 388–394.
Hutley, M. (1982). *Diffraction Gratings*. London: Academic Press.
Jark, W. (2019). *J. Synchrotron Rad.* **26**, 1181–1191.
Kunz, C., Haensel, R. & Sonntag, B. (1968). *J. Opt. Soc. Am.* **58**, 1415–1416.
Lukirskii, A. P. & Savinov, E. P. (1963). *Opt. Spectrosc.* **14**, 147–151.
Nevière, M., Vincent, P. & Petit, R. (1974). *Nouv. Rev. Opt.* **5**, 65–77.
Petersen, H. (1982). *Opt. Commun.* **40**, 402–406.
Petersen, H., Jung, C., Hellwig, C., Peatman, W. B. & Gudat, W. (1995). *Rev. Sci. Instrum.* **66**, 1–14.
Schäfers, F. (2008). *Modern Developments in X-ray and Neutron Optics. Springer Series in Optical Science*, edited by A. Erko, M. Idir, T. Krist and A. G. Michette, Vol. 137. Berlin, Heidelberg: Springer.
Sokolov, A., Huang, Q., Senf, F., Feng, J., Lemke, S., Alimov, S., Knedel, J., Zeschke, T., Kutz, O., Seliger, T., Gwalt, G., Schäfers, F., Siewert, F., Kozhevnikov, I. V., Qi, R., Zhang, Z., Li, W. & Wang, Z. (2019). *Opt. Express*, **27**, 16833–16846.
Voronov, D. L., Gullikson, E. M. & Padmore, H. A. (2018). *Opt. Express*, **26**, 22011–22018.